doi:10.1093/jmcb/mjs034
Published online June 21, 2012

Article

Protocadherin clusters and cell adhesion kinase regulate dendrite complexity through Rho GTPase

Lun Suo[1,2], Huinan Lu[1,2], Guoxin Ying[3], Mario R. Capecchi[3,4], and Qiang Wu[1,2,*]

[1] Key Laboratory of Systems Biomedicine (Ministry of Education), Center for Comparative Medicine, Institute of Systems Biomedicine, Shanghai Jiao Tong University, Shanghai 200240, China
[2] State Key Laboratory of Oncogenes and Related Genes, Shanghai Cancer Institute, Renji Hospital, School of Medicine, Shanghai Jiao Tong University, Shanghai 200240, China
[3] Department of Human Genetics, University of Utah Medical School, Salt Lake City, UT 84112, USA
[4] Howard Hughes Medical Institute, University of Utah, Salt Lake City, UT 84112, USA
* Correspondence to: Qiang Wu, E-mail: qwu123@gmail.com

Dendritic patterning and spine morphogenesis are crucial for the assembly of neuronal circuitry to ensure normal brain development and synaptic connectivity as well as for understanding underlying mechanisms of neuropsychiatric diseases and cognitive impairments. The Rho GTPase family is essential for neuronal morphogenesis and synaptic plasticity by modulating and reorganizing the cytoskeleton. Here, we report that protocadherin (*Pcdh*) clusters and cell adhesion kinases (CAKs) play important roles in dendritic development and spine elaboration. The knockout of the entire *Pcdh*α cluster results in the dendritic simplification and spine loss in CA1 pyramidal neurons *in vivo* and in cultured primary hippocampal neurons *in vitro*. The knockdown of the whole *Pcdh*γ cluster or in combination with the *Pcdh*α knockout results in similar dendritic and spine defects *in vitro*. The overexpression of proline-rich tyrosine kinase 2 (*Pyk2*, also known as CAKβ, RAFTK, FAK2, and CADTK) recapitulates these defects and its knockdown rescues the phenotype. Moreover, the genetic deletion of the *Pcdh*α cluster results in phosphorylation and activation of Pyk2 and focal adhesion kinase (Fak) and the inhibition of Rho GTPases *in vivo*. Finally, the overexpression of *Pyk2* leads to inactivation of Rac1 and, conversely, the constitutive active Rac1 rescues the dendritic and spine morphogenesis defects caused by the knockout of the *Pcdh*α cluster and the knockdown of the *Pcdh*γ cluster. Thus, the involvement of the Pcdh-CAK-Rho GTPase pathway in the dendritic development and spine morphogenesis has interesting implications for proper assembly of neuronal connections in the brain.

Keywords: cell adhesion kinase (CAK), dendrite, protocadherin, Rho GTPase

Introduction

The chemoaffinity hypothesis posits that the expression of specific combinations of diverse transmembrane tagging proteins endows neurons with a proper assembly of neural circuitry (Sperry, 1963; Hattori et al., 2008; Zipursky and Sanes, 2010). The precise wiring of complex neural circuits requires the development and maintenance of elaborate dendritic and spine patterns (Jan and Jan, 2010). To efficiently process information, vertebrate brains evolve and develop with fascinating morphological diversities of thousands of neuronal types with distinctive dendritic trees (Cajal, 1909; Jan and Jan, 2010). These trees are formed from repeated branch addition, stabilization, and extension of the initial outgrowth of dendrites from the soma (Scott and Luo, 2001; Van Aelst and Cline, 2004; Jan and Jan, 2010). Improper dendritic development underlies autism spectrum disorders and mental retardation, whereas defects in spine morphogenesis cause neuropsychiatric diseases such as major depressive disorders, schizophrenia, and dementia (Govek et al., 2005; Jan and Jan, 2010; Lin and Koleske, 2010). Indeed, these diverse and complex neuropsychiatric disorders appear to share certain symptom profiles and to have overlapping underlying genetic mechanisms (Hyman, 2008) such as deficiency in cadherin pathways (Yagi and Takeichi, 2000; Pedrosa et al., 2008; Singh et al., 2009).

Among diverse regulators of dendritic growth and spine morphogenesis are members of the cadherin cell adhesion superfamily proteins (Ye and Jan, 2005; Takeichi, 2007; Lin and Koleske, 2010) and their signaling pathways (Yu and Malenka, 2003). Protocadherin (Pcdh) proteins constitute the largest subfamily of the cadherin superfamily (Yagi and Takeichi, 2000; Zipursky and Sanes, 2010). There are three closely linked clusters of human *Pcdh* genes, designated α, β, and γ, which are arrayed in tandem in a single chromosomal locus (Figure 1A; Wu and Maniatis, 1999). *Pcdh*α and γ clusters each contain more than a dozen variable exons (14 α and 22 γ) followed by a single set of three small constant exons. Each variable exon is alternatively spliced to the common set of constant exons to generate diverse mRNAs that encode large numbers of Pcdh proteins, which share

Received April 4, 2012. Revised May 31, 2012. Accepted June 11, 2012.
© The Author (2012). Published by Oxford University Press on behalf of *Journal of Molecular Cell Biology*, IBCB, SIBS, CAS. All rights reserved.

Downloaded from https://academic.oup.com/jmcb/article/4/6/362/849369 by guest on 16 August 2022

the same cytoplasmic domain in each cluster (Tasic et al., 2002; Wang et al., 2002a). Genetic studies demonstrated that the γ cluster is required for the survival of spinal interneurons (Wang et al., 2002b). In contrast, mice with the deletion of the entire α cluster or its constant region are viable and fertile (Wu et al., 2007; Hasegawa et al., 2008). Pcdhs are expressed in a combinatorial and cell-specific expression pattern in the central nervous system (Kohmura et al., 1998; Wang et al., 2002b; Zou et al., 2007). The exceptional molecular diversity, largely synaptic localization, isoform-specific homophilic adhesive property, and cell-specific expression pattern suggest that Pcdhs play an important role for the assembly of neural circuitry in the vertebrate brain (Kohmura et al., 1998; Shapiro and Colman, 1999; Wu and Maniatis, 1999; Wu et al., 2001; Wu, 2005; Zou et al., 2007; Lefebvre et al., 2008; Katori et al., 2009; Schreiner and Weiner, 2010; Zipursky and Sanes, 2010). However, the mechanisms by which the *Pcdh* clusters ensure a normal assembly of complex neuronal connections remain elusive.

Recently two cell adhesion kinases (CAKs), Pyk2 (proline-rich tyrosine kinase 2) and Fak (focal adhesion kinase), were shown to bind to clustered α and γ proteins (Chen et al., 2009). These two non-receptor tyrosine kinases play important roles in various physiological and pathological processes in non-neuronal cells (Dikic et al., 1996; Avraham et al., 2000; Lietha et al., 2007; Tomar and Schlaepfer, 2009; Schaller, 2010). In contrast, very little is known about their precise functions in neurons (Lev et al., 1995; Derkinderen et al., 1996; Girault et al., 1999; Hsin et al., 2010). Here, we demonstrate that the deletion of the *Pcdhα* cluster by trans-allelic recombination (αKO: *Pcdhα* cluster knockout) *in vivo* and the knockdown of the *Pcdhγ* cluster by RNAi (γKD: *Pcdhγ* cluster knockdown) *in vitro* result in dendritic simplification and spine loss. The overexpression of *Pyk2* recapitulates and the knockdown of *Pyk2* rescues these dendritic developmental defects. Moreover, we provide evidence that the deletion of the *Pcdhα* cluster results in the activation of membrane-associated CAKs as well as the inactivation of the small GTPase Rac1 and RhoA *in vivo*. Together, we conclude that α and γ clusters regulate the dendritic development and spine morphogenesis through a signaling cascade involving the Pyk2-Rac1 pathway.

Results

Dendritic defects in αKO and γKD neurons

To determine the expression patterns of the α cluster *in vivo*, we inserted a CFP reporter in frame at the end of the *Pcdhα* constant coding region (Figure 1B) and found that the clustered Pcdhα proteins are expressed in hippocampus at P1, P3, and P7, especially in the CA1 and CA3 regions (Figure 1C and data not shown). In cultured primary hippocampal neurons, punctuate signals were observed throughout the soma, dendrites, and axons (Figure 1D and E). Costaining with MAP2 and Tau antibodies confirmed its dendritic and axonal localization (data not shown). In conjunction with dendritic expression of Pcdhγ proteins (Phillips et al., 2003), it is suggested that α and γ proteins may function in dendritic development.

To assess the function of α and γ clusters in dendritic development, we cultured E18.5 hippocampal neurons from the αKO mice (Wu et al., 2007) and transfected with γKD constructs (Figure 1F–I; Supplementary Figure S1). In developing neurons, the quantification demonstrated that TDBTN (total dendritic branch tip number) in either αKO or γKD, or the combination, is significantly decreased (Figure 1O). In addition, the TDBL (total dendritic branch length) and the number of primary dendrites are significantly decreased in neurons with γKD or combined with αKO (Figure 1N and Q). Moreover, the ADBL (average dendritic branch length) is significantly increased in αKO (Figure 1P). Sholl analysis revealed that dendritic patterns are simplified with γKD or combined with αKO (Figure 1R). Finally, αKO results in a significant decrease in dendritic filopodia; however, γKD causes a significant increase in dendritic filopodia (Figure 1V and data not shown). In mature neurons, both αKO and γKD cause the spine loss (Figure 1J–M and S). In particular, there are striking losses of typical mushroom- and stub-shaped dendritic spines with either αKO or γKD, or the combination (Figure 1J–M and W). The quantification of the spine length and the width revealed that they decrease significantly with the exception of αKO for the spine length (Figure 1T and U). These experiments support the hypothesis that the α and γ clusters are required for dendritic and spine morphogenesis.

Our *in-vitro* data suggest a potential role of the α cluster in dendrite and spine morphogenesis *in vivo*. To this end, we performed the Golgi staining and 3D reconstruction of the entire individual CA1 pyramidal neurons from the control (Figure 2A) and homozygous (Figure 2B) littermates of the α cluster deletion mice. The quantification of the reconstructed confocal images revealed a significant reduction in the number of branch points (bifurcations; Figure 2C) as well as of segments (Figure 2D) between branch points in the absence of the α cluster. Sholl analysis demonstrated a significant simplification of dendritic arbor complexity in neurons without members of the α cluster (Figure 2E). In addition, the quantification of spine numbers of confocal images of dendritic segments (Figure 2F and G) revealed a significant reduction in the spine density in homozygotes (Figure 2H). However, there is no significant difference in the spine length and spine width between homozygotes and controls (Figure 2I and J). Taken together, these data demonstrated a role of the α cluster in dendrite and spine morphogenesis *in vivo*.

To further confirm the role of clustered *Pcdhs* in dendritic development, we transfected a dominant-negative construct encoding a myristylated α or γ constant region (myr-α-CR or myr-γ-CR; Figure 3A–D). The overexpression of these constant intracellular domains could sequester the respective cytoplasmic partners, similar to the well-established method of the blocking of β-catenin by overexpression of the intracellular domain of N-cadherin (Yu and Malenka, 2003). Immunostaining indicated that the myristylated domain is localized throughout the cell surface including dendrites at 7 days *in vitro* (DIV; Supplementary Figure S2). The quantification of TDBL, TDBTN, and number of primary dendrites, and Sholl analysis demonstrated significant dendritic developmental defects (Figure 3E–H). In mature neurons, these dominant negative forms induce the spine loss reminiscent of αKO and γKD (Figure 3J–L and N). Immunostaining of synaptophysin, a presynaptic marker, showed that myr-α-CR leads to a dramatic decrease of synapses

Downloaded from https://academic.oup.com/jmcb/article/4/6/362/849369 by guest on 16 August 2022

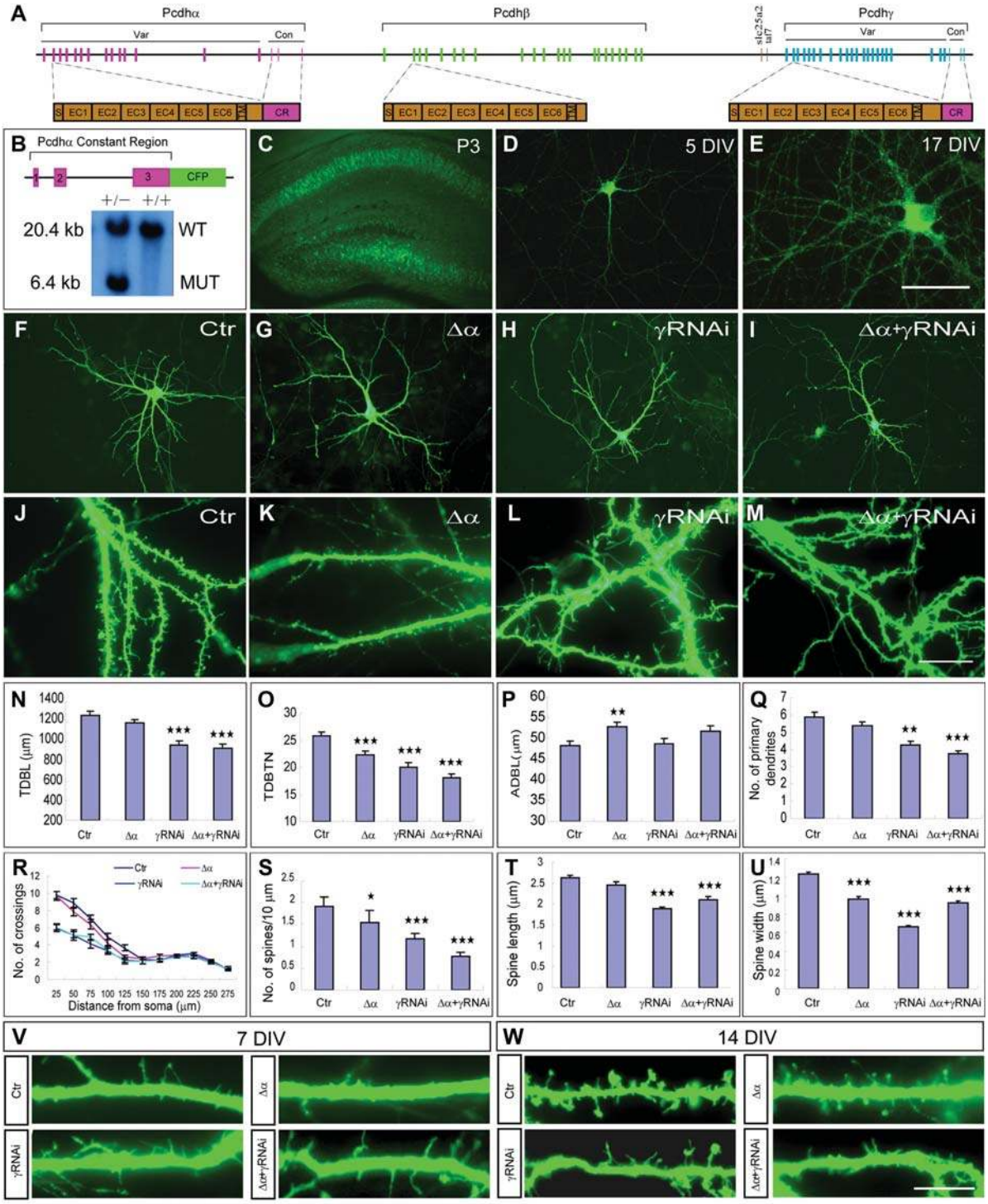

Figure 1 *Pcdhα* and *γ* clusters are required for dendritic development and spine morphogenesis. (**A**) Schematic of the *Pcdh* locus. (**B**) Confirmation of knockin by Southern blot. *Pcdhα* expression patterns in hippocampus (**C**) and in 5 DIV (**D**) or 17 DIV neurons (**E**). The scale bar in **E** represents 400 μm for **C**, 100 μm for **D**, 50 μm for **E**. Representative images of hippocampal neurons in the control (**F** and **J**) and Δ*α* mice (**G** and **K**) or with γRNAi (**H**, **I**, **L**, and **M**) in 7 DIV (**F**–**I**) and 14 DIV (**J**–**M**). Scale bar in **M**, 100 μm for **F**–**I**; 20 μm for **J**–**M**. The quantification of TDBL (**N**), TDBTN (**O**), ADBL (**P**), number of primary dendrites (**Q**), and Sholl analysis (**R**) of 7 DIV neurons (Ctr, $n = 81$; Δ*α*, $n = 87$; γRNAi, $n = 75$; Δ*α* + γRNAi, $n = 75$). The quantification of the spine density (**S**) (Ctr, $n = 98$; Δ*α*, $n = 94$; γRNAi, $n = 77$; Δ*α* + γRNAi, $n = 77$), spine length (**T**), and width (**U**) (Ctr, $n = 335$ spines of 26 dendritic segments; Δ*α*, $n = 188/15$; γRNAi, $n = 442/28$; Δ*α* + γRNAi, $n = 278/20$) of 14 DIV neurons. Representative images of filopodia (**V**) and spines (**W**) in dendritic segments of 7 and 14 DIV neurons. Scale bar in **W**, 10 μm for **V**, **W**. Data are expressed as the mean ± SEM. $^*P < 0.05$, $^{**}P < 0.01$, $^{***}P < 0.001$.

Downloaded from https://academic.oup.com/jmcb/article/4/6/362/849369 by guest on 16 August 2022

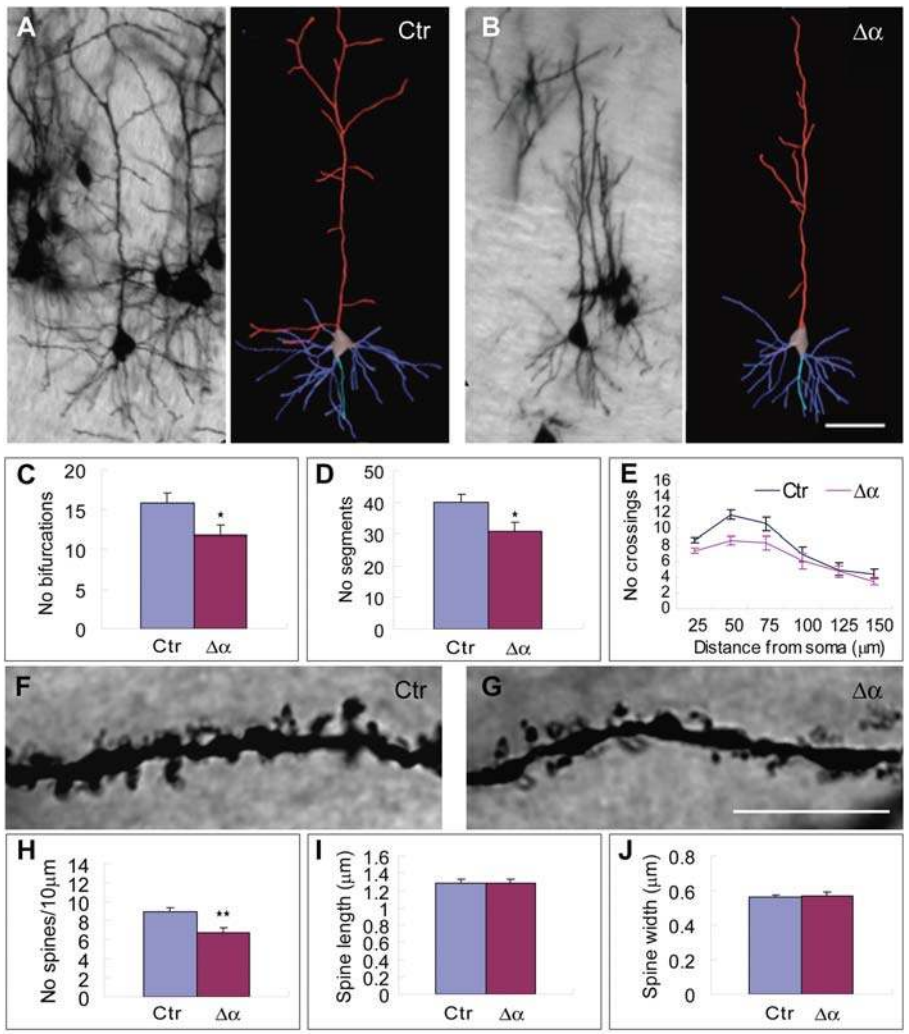

Figure 2 The α cluster is required for dendrite and spine development *in vivo*. The representative Golgi staining of CA1 hippocampal neurons and the reconstructed 3D confocal images from the control (**A**) and homozygous (**B**) littermates of the targeted deletion of the entire α cluster. Scale bar in **B** represents 100 μm for **A** and **B**. Quantification of branch points (bifurcation) (**C**), the number of segments (**D**) between branch points, and Sholl analysis (**E**) (Ctr, $n = 21$; $\Delta\alpha$, $n = 20$). Representative confocal images of the basal dendritic segments from the CA1 pyramidal neurons of the control (**F**) and homozygous (**G**) littermate mice. The scale bar in **G** represents 10 μm for **F** and **G**. The quantification of the spine density (**H**), spine length (**I**), and width (**J**) (Ctr, $n = 499$ spines of 20 dendritic segments; $\Delta\alpha$, $n = 419/23$). Data are expressed as the mean ± SEM. $^*P < 0.05$, $^{**}P < 0.01$.

(Supplementary Figure S3). It is well known that α and γ proteins form complexes in *cis* (Murata et al., 2004; Han et al., 2010; Schreiner and Weiner, 2010). Thus, the striking similarity of phenotypes upon transfection of myr-α-CR or myr-γ-CR suggests that each interferes with functions of both α and γ clusters. Together, these dominant-negative experiments confirmed that α and γ clusters function in dendritic development and spine morphogenesis (Figure 3).

Overexpression of Pyk2 causes dendritic defects

To explore mechanisms by which α and γ clusters regulate dendritic development, we cloned and overexpressed *Pyk2* and *Fak* in developing and mature neurons (Supplementary Figure S4). The overexpression of *Pyk2* but not *Fak* recapitulates the dendritic simplification and spine loss observed from αKO and γKD (Figure 4; Supplementary Figure S5). Moreover, the overexpression of the kinase-dead Pyk2 K457A mutant does not recapitulate these defects (Figure 4E and J–L; Supplementary Figure S5). Thus, the kinase activity of Pyk2 is required for dendritic development.

The recapitulated defects are also dependent on the autophosphorylation of Pyk2 Y402 and subsequent phosphorylation of Y881, but not Y579 and Y580 (Figure 4A, D, and F–M; Supplementary Figure S5). This is consistent with different roles of phosphorylated Y881 and Pyk2 Y579 and Y580 (Avraham et al., 2000). Phosphorylated Y881 interacts with the SH2 domain of the adaptor protein Grb2 (Lev et al., 1995; Dikic et al., 1996), which regulates cytoskeletal reorganization (Avraham et al., 2000). Thus, the Pyk2-Grb2 pathway may be involved in regulating dendritic simplification by α and γ clusters. However, the overexpression of mutants Y579F, Y580F, or Y881F still recapitulates the spine morphogenesis phenotype (Figure 4N–Q and V–X). This suggested that signaling through

Downloaded from https://academic.oup.com/jmcb/article/4/6/362/849369 by guest on 16 August 2022

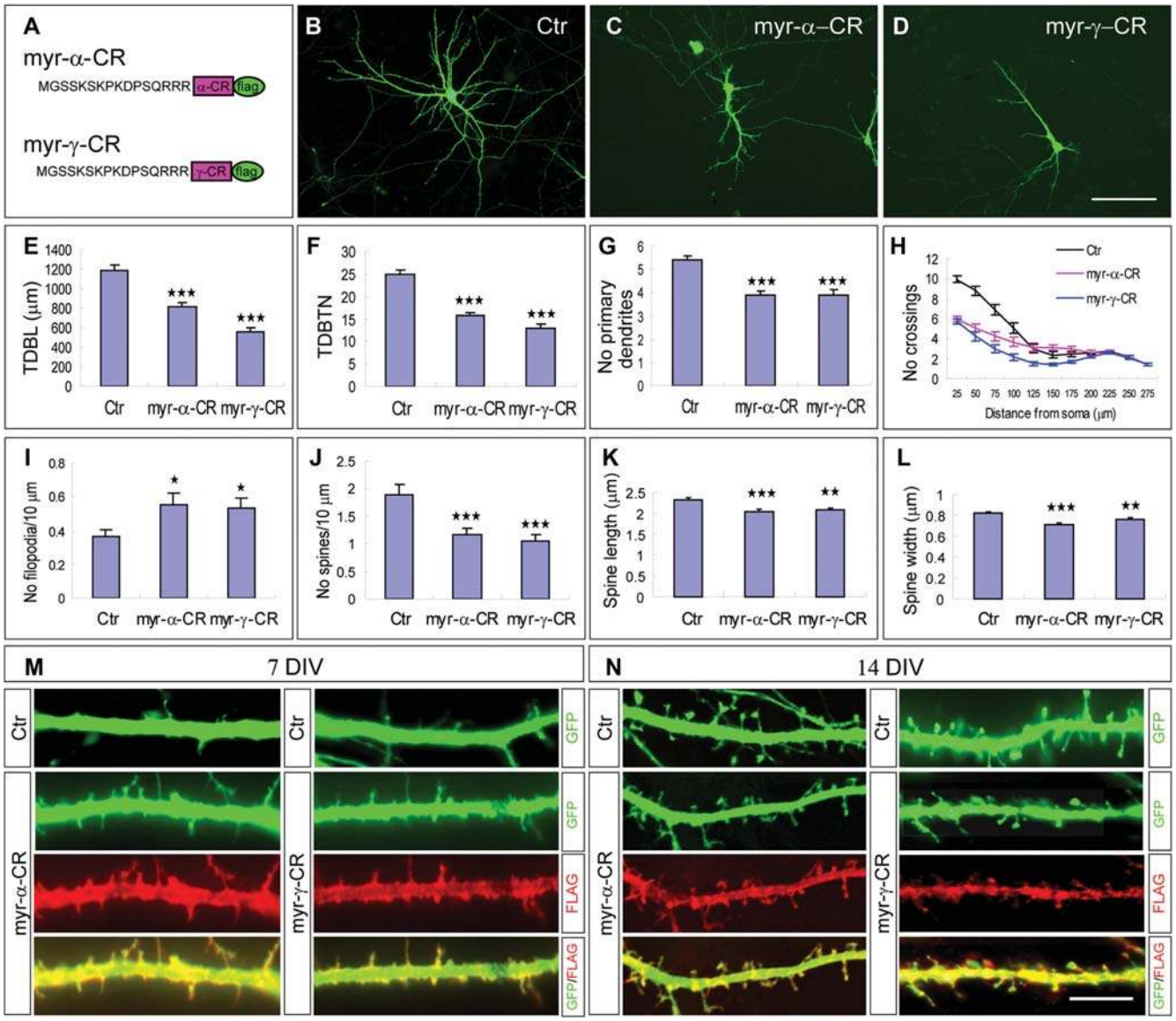

Figure 3 Dominant-negative forms of myr-α-CR and myr-γ-CR recapitulate phenotypes of dendritic development and spine morphogenesis. (**A**) Schematics of myr-α-CR and myr-γ-CR myristylated membrane-attaching constructs. Representative images of 7 DIV hippocampal neurons cotransfected GFP with Mock (**B**), myr-α-CR (**C**), or myr-γ-CR (**D**). Scale bar in **D** represents 100 μm for **B**–**D**. The quantification of TDBL (**E**), TDBTN (**F**), number of primary dendrites (**G**), and Sholl analysis (**H**) of 7 DIV hippocampal neurons (Ctr, $n = 40$; myr-α-CR, $n = 35$; myr-γ-CR, $n = 38$). (**I**) The quantification of density of filopodia of 7 DIV dendritic segments (Ctr, $n = 43$; myr-α-CR, $n = 44$; myr-γ-CR, $n = 37$). (**J**) The quantification of the spine density of 14 DIV dendritic segments (Ctr, $n = 31$; myr-α-CR, $n = 47$; myr-γ-CR, $n = 29$). The quantification of the spine length (**K**) and width (**L**) of 14 DIV neurons (Ctr, $n = 508$ spines of 33 dendritic segments; myr-α-CR, $n = 449/37$; myr-γ-CR, $n = 430/31$). Representative images of 7 DIV (**M**) and 14 DIV (**N**) neuronal segments cotransfected with GFP and Mock, myr-α-CR or myr-γ-CR. The scale bar in **N** represents 10 μm for **M** and **N**. Data are expressed as the mean ± SEM. $^*P < 0.05$, $^{**}P < 0.01$, $^{***}P < 0.001$.

phosphorylation of Y402, but not of Y579, Y580, or Y881, is important for spine morphogenesis.

Pyk2 knockdown rescues dendritic defects

To analyze the epistatic relationship between *Pyk2* and *Pcdhs*, we designed an efficient *Pyk2* shRNA (RNAi3) assay to determine whether suppressed Pyk2 activity would rescue the dendritic phenotype resulting from compromised *Pcdh* clusters (Supplementary Figure S6). Strikingly, the quantification of TDBL, TDBTN, number of primary dendrites, as well as Sholl analysis revealed that the *Pyk2* knockdown does rescue the dendritic simplification phenotype resulting from αKO and γKD (Figure 5A–H). In mature neurons, the quantification of the spine density, length, and width revealed that the knockdown of *Pyk2* also rescues the spine defects of αKO and γKD (Figure 5I–O). These rescue experiments demonstrated that *Pyk2* acts downstream of α and γ clusters to regulate dendritic development.

Pcdhs regulate dendritic development via Rho GTPases

Owning to an essential role of the Rho GTPase family in dendritic development (Scott and Luo, 2001; Govek et al., 2005), we investigated whether they are involved in the regulation of

Downloaded from https://academic.oup.com/jmcb/article/4/6/362/849369 by guest on 16 August 2022

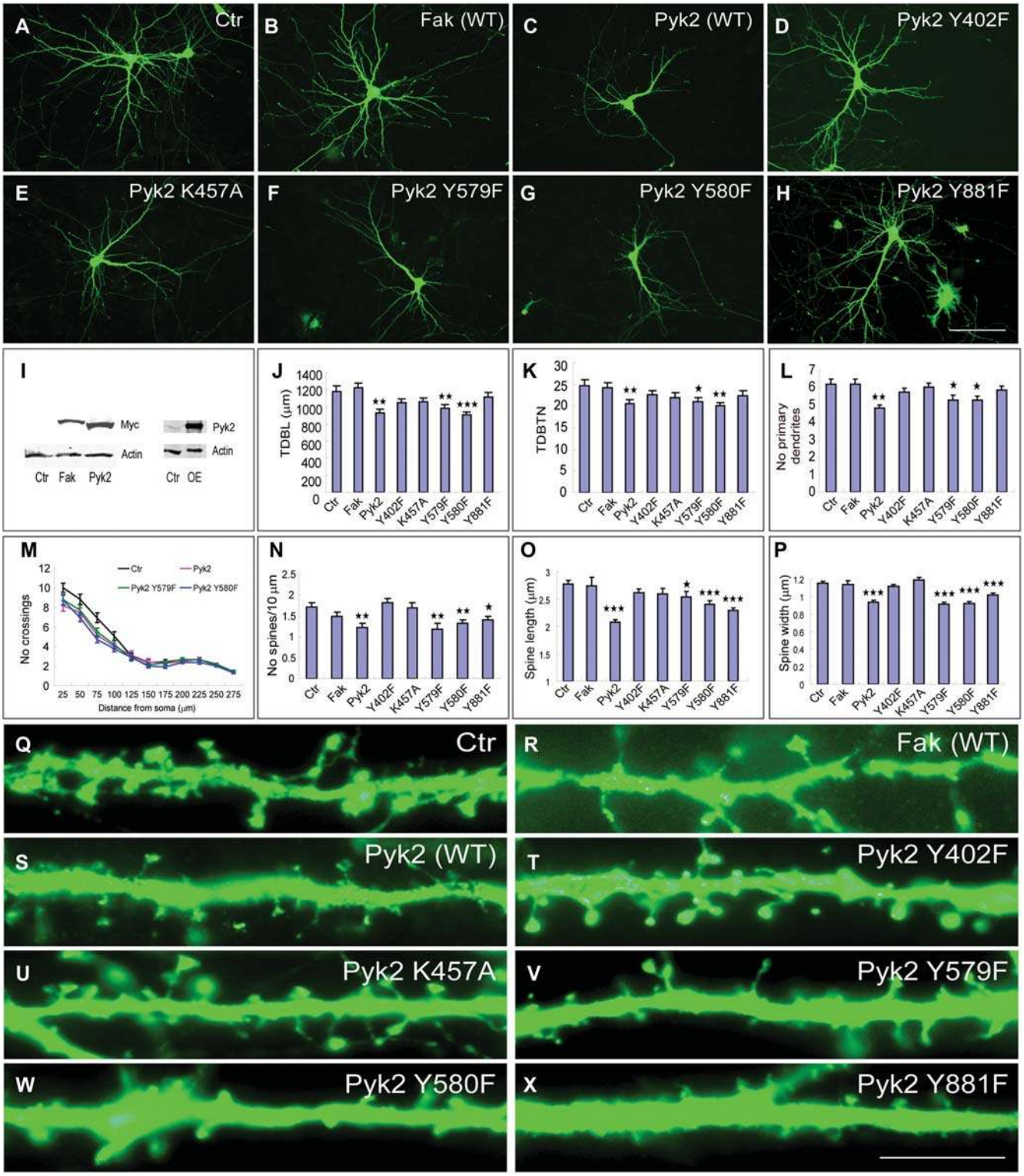

Figure 4 *Pyk2* functions in dendritic development. Representative images of 7 DIV neurons cotransfected with GFP and Mock (**A**), Fak (**B**), Pyk2 (**C**), or Pyk2 mutants Y402F (**D**), K457A (**E**), Y579F (**F**), Y580F (**G**), Y881F (**H**). Scale bar in **H**, 100 μm for **A**–**H**. (**I**) Western blots showing the overexpression (OE) of Fak and Pyk2 proteins. The quantification of TDBL (**J**), TDBTN (**K**), number of primary dendrites (**L**) (Ctr, $n = 40$; Fak, $n = 42$; Pyk2, $n = 40$; Y402F, $n = 39$; K457A, $n = 38$; Y579F, $n = 40$; Y580F, $n = 40$; Y881F, $n = 40$), and Sholl analysis (**M**) of 7 DIV neurons (Ctr, $n = 40$; Pyk2, $n = 40$; Y579F, $n = 40$; Y580F, $n = 40$). (**N**–**P**) The quantification of the spine density (Ctr, $n = 46$; Fak, $n = 32$; Pyk2, $n = 37$; Y402F, $n = 39$; K457A, $n = 32$; Y579F, $n = 36$; Y580F, $n = 42$; Y881F, $n = 34$), spine length, and width of 14 DIV hippocampal neurons (Ctr, $n = 370/31$; Fak, $n = 192/24$; Pyk2, $n = 273/21$; Y402F, $n = 376/30$; K457A, $n = 204/16$; Y579F, $n = 195/13$; Y580F, $n = 224/18$; Y881F, $n = 397/35$). The corresponding images of branch segments of 14 DIV neurons (**Q**–**X**). Scale bar in **X** represents 10 μm for **Q**–**X**.

Downloaded from https://academic.oup.com/jmcb/article/4/6/362/849369 by guest on 16 August 2022

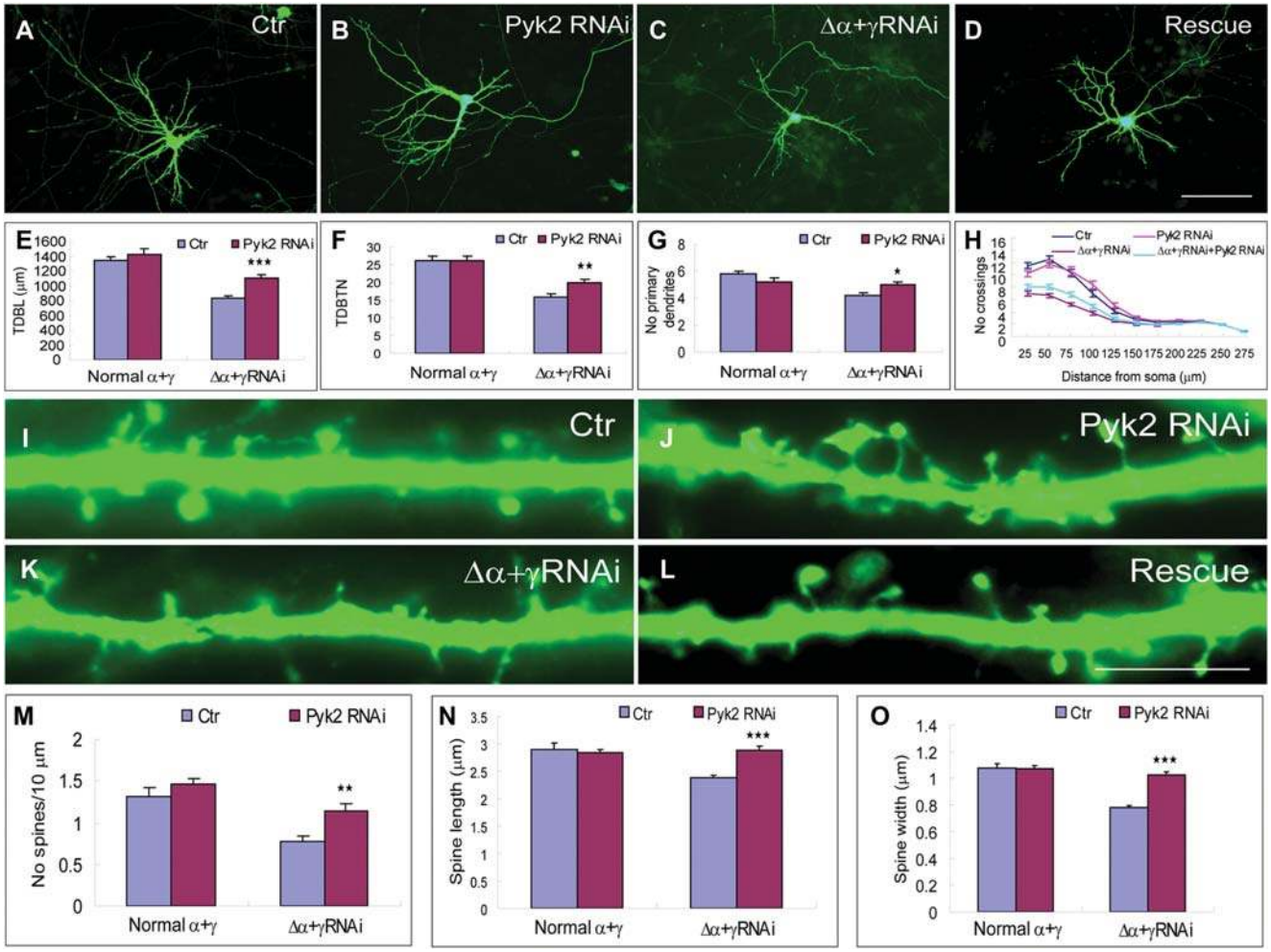

Figure 5 The knockdown of *Pyk2* rescues dendritic simplification and spine loss of αKO and γKD. Representative images of 7 DIV neurons of wild type cotransfected with GFP and Mock (**A**) or *Pyk2* RNAi (**B**) constructs, and of αKO and γKD and cotransfected with GFP and Mock (**C**) or *Pyk2* RNAi rescue (**D**) constructs. Scale bar in **D**, 100 μm for **A**–**D**. The quantification of TDBL (**E**), TDBTN (**F**), number of primary dendrites (**G**), and Sholl analysis (**H**) (Ctr, $n = 40$; *Pyk2* RNAi, $n = 40$; $\Delta\alpha + \gamma$RNAi, $n = 40$; Rescue, $n = 40$). Corresponding images of dendritic segments of 14 DIV neurons (**I**–**L**). Scale bar in **L** represents 10 μm for **I**–**L**. The quantification of the spine density (**M**) (Ctr, $n = 30$; *Pyk2* RNAi, $n = 33$; $\Delta\alpha + \gamma$RNAi, $n = 39$; Rescue, $n = 34$), spine length (**N**), and width (**O**) (Ctr, $n = 138/25$; *Pyk2* RNAi, $n = 317/33$; $\Delta\alpha + \gamma$RNAi, $n = 413/47$; Rescue, $n = 333/34$).

dendritic simplification and spine morphogenesis by α and γ clusters. To this end, we disrupted their activity with the Rac1-specific inhibitor NSC23766 or the Rho-associated kinase (ROCK) specific inhibitor Y-27632. We found that Rac1 but not ROCK inhibition recapitulates the dendritic simplification of αKO and γKD (Figure 6A–K). Consistent with previous report, ROCK inhibition on its own does not affect dendritic development (Figure 6A, B, D, and H–K; Nakayama et al., 2000). However, combined with αKO and γKD, ROCK inhibition causes a significant increase in ADBL (Figure 6H). In mature neurons, Rac1 inhibition recapitulates spine defects of αKO and γKD (Figure 6L–T). Combined with αKO and γKD, ROCK inhibition causes a significant increase in the spine length (Figure 6M–S). Therefore, Pcdhs may regulate the cytoskeletal reorganization through Rho GTPases.

To confirm that α and γ clusters and *CAK* regulate the dendritic development through *Rac1*, we used Rac1V12 (constitutively active Rac1) to rescue the phenotype. Previous transgenic and transfected expression of Rac1V12 has been reported to result in a slight simplification of dendritic morphology, but a significant loss of dendritic spines (Luo et al., 1996; Nakayama et al., 2000). Consistent with these studies, the expression of Rac1V12 does not cause a significant dendritic simplification (Figure 7A–H). Strikingly, Rac1V12 rescues the dendritic developmental defects resulting from αKO and γKD. Moreover, Rac1V12 causes a significant spine loss in mature neurons (Nakayama et al., 2000), whereas it rescues spine length and width defects of αKO and γKD (Figure 7I–O). These experiments demonstrated that clustered *Pcdhs* regulate the dendritic and spine morphogenesis through *Rac1*.

Pcdhs inhibit CAKs and thus activate Rho GTPases

To determine whether the expression levels of CAKs and Rho GTPases are altered in αKO mice, we performed Western blots using brain extracts of αKO mice (Figure 8) and found a significant increase in phosphorylation of Pyk2 pY402 and Fak pY397 in

Downloaded from https://academic.oup.com/jmcb/article/4/6/362/849369 by guest on 16 August 2022

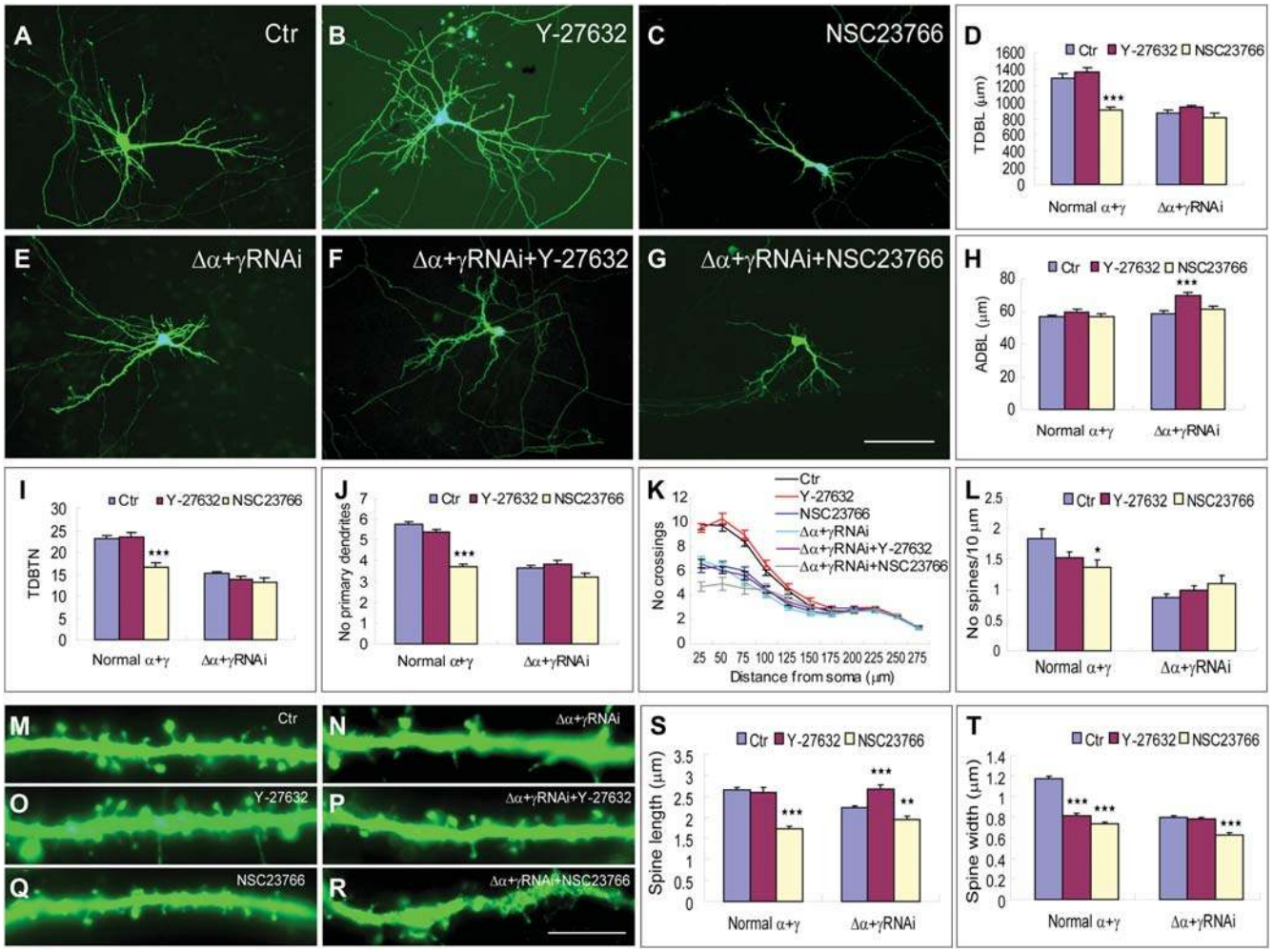

Figure 6 *Rac1* but not *ROCK* inhibition recapitulates the dendritic and spine development phenotype of αKO and γKD. Representative images of 7 DIV neurons transfected with GFP (**A**) and applied with Y-27632 (**B**) or NSC23766 (**C**), and from αKO and γKD (**E**) and applied with Y-27632 (**F**) or NSC23766 (**G**). Scale bar in **G** represents 100 μm for **A**–**C** and **E**–**G**. The quantification of TDBL (**D**), ADBL (**H**), TDBTN (**I**), number of primary dendrites (**J**), and Sholl analysis (**K**) (Normal $\alpha+\gamma$: Ctr, $n=69$; Y-27632, $n=67$; NSC23766, $n=65$; $\Delta\alpha+\gamma$RNAi: Ctr, $n=76$; Y-27632, $n=52$; NSC23766, $n=26$). Corresponding images of branch segments (**M**–**R**). Scale bar in **R**, 10 μm for **M**–**R**. The quantification of the spine density (**L**) (Normal $\alpha+\gamma$: Ctr, $n=29$; Y-27632, $n=18$; NSC23766, $n=23$; $\Delta\alpha+\gamma$RNAi: Ctr, $n=56$; Y-27632, $n=28$; NSC23766, $n=31$), spine length (**S**), and width (**T**) (Normal $\alpha+\gamma$: Ctr, $n=398/31$; Y-27632, $n=148/19$; NSC23766, $n=308/17$; $\Delta\alpha+\gamma$RNAi: Ctr, $n=684/20$; Y-27632, $n=260/27$; NSC23766, $n=122/8$).

membrane fractions (Figure 8C and F). This demonstrated that the α cluster inhibits phosphorylation of CAKs *in vivo*. Moreover, the activated forms of Rac1 (Rac1-GTP) and RhoA (RhoA-GTP) decrease significantly (Figure 8G and H).

To determine if the overexpression of *Pyk2* alters the activity of Rho GTPases in cell culture, we overexpressed it in HEK293 cells and found that *Pyk2* overexpression results in decrease in Rac1-GTP (Figure 8I). This suggested that αKO causes decrease in Rac1-GTP through Pyk2 activation. In conjunction with *Pyk2* inhibition by the γ cluster (Chen et al., 2009), we concluded that the disruption of α and γ clusters causes dendritic simplification and spine loss through *Pyk2*. Thus, *Pcdhs* regulate dendritic and spine morphogenesis through inhibition of *Pyk2*, leading to the localized activation of Rac1. Interestingly, the *Fak* knockdown causes dendritic simplification, especially a significant decrease in ADBL (Supplementary Figure S7). In conjunction with functional characterization of Pcdhs (Figure 1) and CAK (Figures 4 and 5), this suggested that clustered *Pcdhs* function in dendritic development through CAK and small GTPase.

A Pcdh-Pyk2-Rac1 pathway for dendritic development

We propose a model for α and γ clusters to regulate the dendritic and spine morphogenesis by activating Rac1 through inhibiting Pyk2 (Figure 9). Both α and γ clusters inhibit Pyk2 (Figure 8; Chen et al., 2009). Pyk2 inhibits Rac1 because the overexpression of *Pyk2* leads to decrease in activated Rac1 (Figure 8I). The inhibition of Rac1 recapitulates the dendritic development of αKO and γKD (Figure 6). Rac1V12 rescues dendritic simplification (Figure 7A–H) and spine size (Figure 7I–L, N, and O). Thus, the clustered *Pcdhs* regulate the dendritic complexity via Pyk2 and Rac1.

Downloaded from https://academic.oup.com/jmcb/article/4/6/362/849369 by guest on 16 August 2022

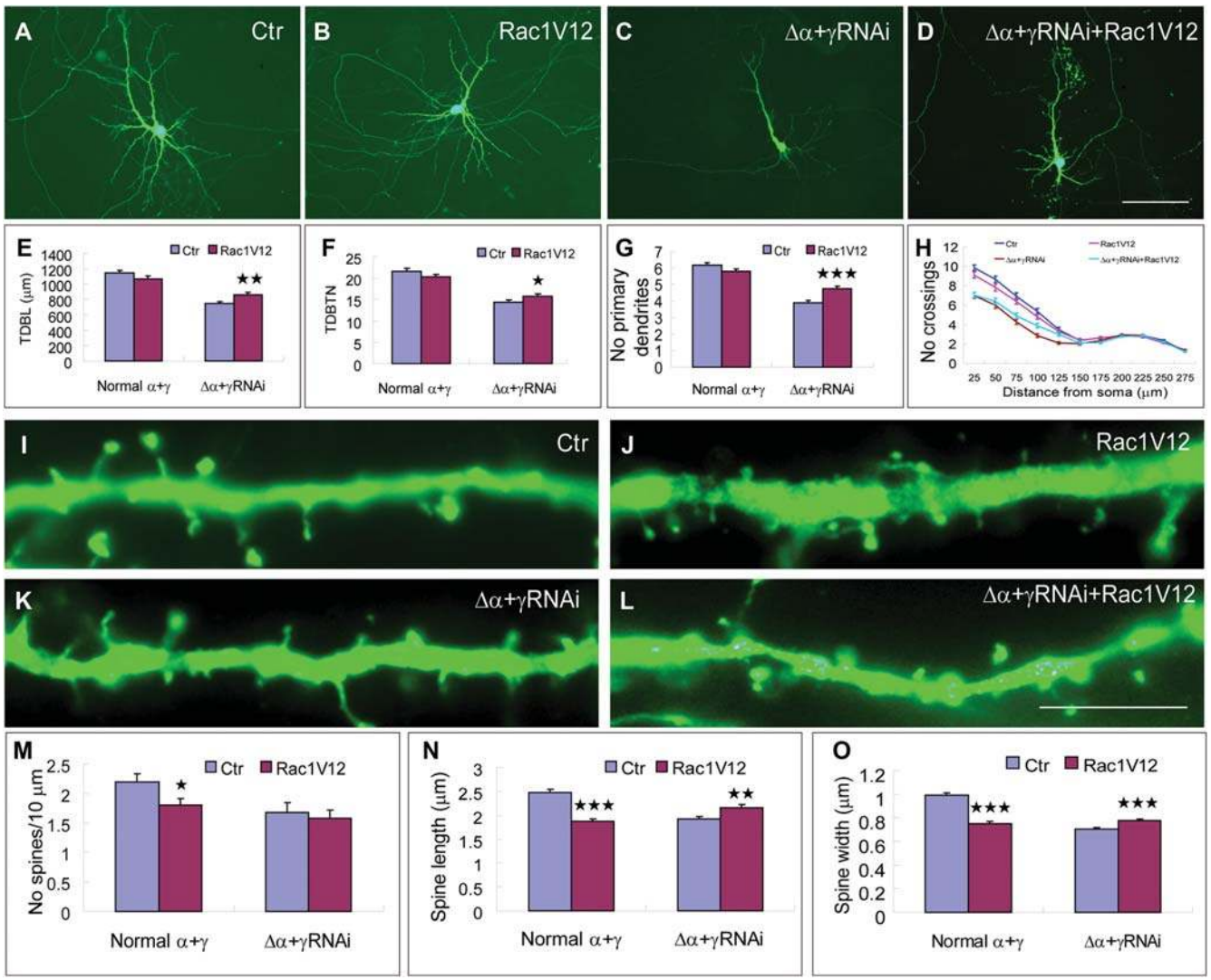

Figure 7 Rac1V12 rescues the dendritic development of αKO and γKD. Representative images of 7 DIV neurons of wild type cotransfected with GFP and Mock (**A**) or Rac1V12 (**B**) constructs, and of αKO and γKD and cotransfected with GFP and Mock (**C**) or Rac1V12 (**D**). Scale bar in **D**, 100 μm for **A**–**D**. The quantification of TDBL (**E**), TDBTN (**F**), number of primary dendrites (**G**), and Sholl analysis (**H**) at 7 DIV (Ctr, $n = 89$; Rac1V12, $n = 84$; $\Delta\alpha + \gamma$RNAi, $n = 80$; $\Delta\alpha + \gamma$RNAi + Rac1V12, $n = 82$). Corresponding images of dendritic segments at 14 DIV (**I**–**L**). Scale bar in **L**, 10 μm for **I**–**L**. The quantification of the spine density (**M**) (Ctr, $n = 32$; Rac1V12, $n = 29$; $\Delta\alpha + \gamma$RNAi, $n = 29$; $\Delta\alpha + \gamma$RNAi + Rac1V12, $n = 17$), spine length (**N**), and width (**O**) (Ctr, $n = 372/27$; Rac1V12, $n = 378/23$; $\Delta\alpha + \gamma$RNAi, $n = 490/26$; $\Delta\alpha + \gamma$RNAi + Rac1V12, $n = 265/23$).

Discussion

The mammalian brain contains billions of neurons each with up to 20 000 synapses, resulting in trillions of specific neuronal connections. One of the central problems in understanding normal and pathological development of the brain is to determine how diverse neurons establish and maintain this complex synaptic connectivity. Dendrites equipped with amazing diversities of complex patterning have enormous influences on how neurons establish synaptic connectivity during brain development and how the neural circuitry is remodeled for information integration during memory formation. Both intrinsic genetic programs and extrinsic environmental stimuli influence the development of complex dendritic arborization and spine morphogenesis (Scott and Luo, 2001; Van Aelst and Cline, 2004; Konur and Ghosh, 2005; Ye and Jan, 2005; Jan and Jan, 2010; Lin and Koleske, 2010). Pcdhs, a large family of cadherin-like proteins with striking diversities generated by alternative splicing, have been proposed as neuronal 'identity tags' or 'address codes' in neural circuitry assembly (Shapiro and Colman, 1999; Wu and Maniatis, 1999; Zipursky and Sanes, 2010). *CAKs* may plays important roles in neural development and synaptic plasticity (Lev et al., 1995; Dikic et al., 1996; Girault et al., 1999). However, the mechanisms by which *Pcdhs* and *CAKs* regulate neuronal connectivity have not been determined (Girault et al., 1999; Lamprecht and LeDoux, 2004; Zipursky and Sanes, 2010). Here, we report that *Pcdhα* and *γ* clusters and *CAKs* function in dendritic development and spine morphogenesis and that *Pcdhs* inhibit *CAKs*, leading to the activation of Rho GTPases to regulate cytoskeleton

Downloaded from https://academic.oup.com/jmcb/article/4/6/362/849369 by guest on 16 August 2022

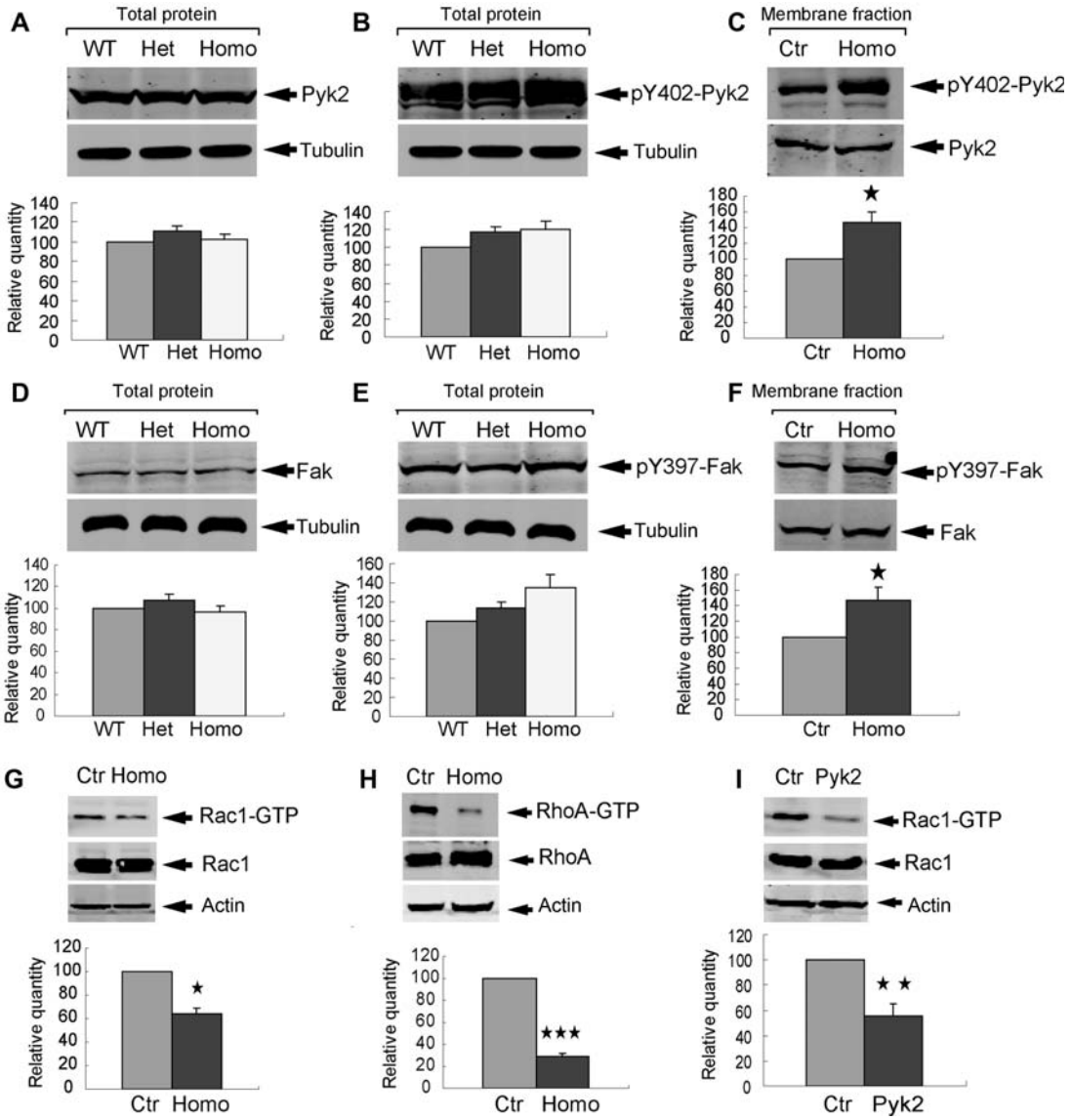

Figure 8 The targeted deletion of the α cluster leads to activation of *Pyk2* and *Fak* as well as the inactivation of *Rac1* and *RhoA in vivo*. Western blots of brain extracts with antibodies against Pyk2 (**A**), Fak (**D**), or phosphorylated forms of pY402-Pyk2 (**B**) and pY397-Fak (**E**). Western blots of membrane fractions with these four antibodies (**C** and **F**) showing augmented phosphorylation of Pyk2 and Fak in homozygous mice. Western blots of total brain extracts or affinity-precipitated active forms of Rac1 (**G**) and RhoA (**H**). The Rac1 (**I**) activation assay in HEK293 cells demonstrates that the overexpression of *Pyk2* leads to inactivation of *Rac1*. Quantifications were normalized with tubulin (**A**, **B**, **D**, **E**), membrane-associated total Pyk2 (**C**) or Fak (**F**), total Rac1 (**G**, **I**) or RhoA (**H**), and shown under each corresponding panel.

reorganization. Herein, we suggest that the Pcdh-CAK-Rho GTPase pathway plays a critical role in dendritic arborization and spine morphogenesis.

Two large families, Dscam and Pcdh, of homophilic cell adhesion proteins with complex genomic organization and cell-specific combinatorial expression patterns have been suggested as candidates for chemoaffinity tags to assemble the extensive diversity of neuronal connections observed in *Drosophila* and vertebrates, respectively (Zipursky and Sanes, 2010). Diverse *Drosophila* Dscam1 proteins are required for self-avoidance of sister dendrites of same neurons and may also play a role in tiling between dendrites of different neurons of same types (Hattori et al., 2008; Jan and Jan, 2010). It has been speculated that diverse Pcdh proteins may play a similar role in vertebrates (Zipursky and Sanes, 2010). However, little is known about the mechanisms by which homophilic adhesion leads to contact-dependent repulsion of self-avoidance and tiling (Hattori et al., 2008; Zipursky and Sanes, 2010). It is intriguing that the clustered *Pcdhs* can potentially achieve adhesion-dependent repulsion through the CAK-Rho GTPase pathway to reorganize the cytoskeleton. Through this mechanism, the diversity of Pcdhs generated by tandem arrayed clusters may be essential for complex dendritic field patterning and proper assembly of synaptic connections in vertebrates.

Members of the α and γ families interact with each other in *cis* through extracelluar and cytoplasmic domain (Murata et al.,

Downloaded from https://academic.oup.com/jmcb/article/4/6/362/849369 by guest on 16 August 2022

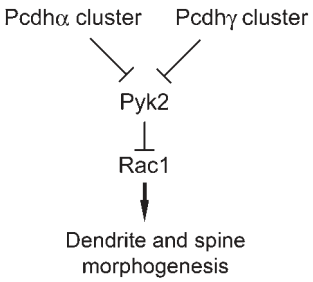

Figure 9 Model depicting the roles of *Pcdhs* and *Pyk2* in regulating dendrite arborization through the Rac1 signaling pathway. The clustered *Pcdh*s are involved in the inhibition of Pyk2 and thus result in the disinhibition of the Rac1, which may lead to assembly of normal dendritic arborization and proper synaptic connectivity.

2004; Schreiner and Weiner, 2010). Their cytoplasmic domains interact with CAKs (Chen et al., 2009). The recapitulation of *Pcdh* phenotype of dendritic simplification and spine loss by *Pyk2* overexpression and its rescue by *Pyk2* knockdown support that *Pyk2* acts downstream of *Pcdhs* to regulate dendritic arborization. Knockout of α or γ clusters leads to the phosphorylation of Y402 (Figure 8; Chen et al., 2009) and the phosphorylated Y402 recruits Src through its SH2 domain (Dikic et al., 1996). The activated Src phosphorylates Y881 (Lev et al., 1995; Avraham et al., 2000). The phosphorylated Pyk2 Y881 (corresponding to Fak Y925) binds the adaptor Grb2 through its SH2 domain (Schlaepfer et al., 1994; Lev et al., 1995; Dikic et al., 1996). Grb2 forms a complex with p190RhoGAP, leading to the p190RhoGAP activation and phosphorylation by the activated Src (Arthur et al., 2000; Zrihan-Licht et al., 2000; Lamprecht et al., 2002). The Pyk2 mutagenesis experiments show that Pyk2 Y402 and Y881 are important for regulating dendritic development. Therefore, the signaling through Pyk2 Y881 is important for Pcdhs to regulate dendritic development. However, the Pyk2 Y881 is not essential for spine morphogenesis since the Pyk2 Y881F mutation does not disrupt its ability to recapitulate the spine loss phenotype. This suggested that dendritic morphogenesis and spine development are different with respect to the dependence on Pyk2 Y881 phosphorylation.

Members of Rho GTPase family are intracellular signaling switches that control the dynamics of actin and microtubule assembly in both neurons and non-neuronal cells (Burridge and Wennerberg, 2004; Govek et al., 2005). Rho GTPases are activated by guanine nucleotide exchange factors (RhoGEFs) and inactivated by GTPase-activating proteins (RhoGAPs; Scott and Luo, 2001; Burridge and Wennerberg, 2004; Van Aelst and Cline, 2004; Jan and Jan, 2010; Lin and Koleske, 2010). Mutations of Rho GTPase regulators and effectors have been associated with nervous system diseases through the alteration of neuronal morphology (Govek et al., 2005; Jan and Jan, 2010). In general, Rac1 regulates actin nucleation and polymerization, whereas the RhoA controls the contractibility of actin cytoskeleton through its downstream effector ROCK (Scott and Luo, 2001; Govek et al., 2005; Jan and Jan, 2010).

In focal adhesions at the leading edge of migratory cells, Fak is a key regulator of the localized RhoGAP and RhoGEF activity (Tomar and Schlaepfer, 2009; Schaller, 2010). RhoA is initially inhibited by phosphorylated p190RhoGAP which is activated by Fak. This leads to increased actin polymerization and cell spreading (PUSH). At later stages, RhoA is activated by p190RhoGEF, resulting in increased cell contractility (PULL). This cyclic inactivation and activation are important for promoting leading edge stability, which is essential for efficient directional cell migration (Tomar and Schlaepfer, 2009). Neurons may utilize similar mechanisms to cyclically inhibit and activate Rho GTPases in growth cones at the dendritic tips and in spines to regulate cytoskeletal dynamics. In the growing tips of dendrites and spines, RhoA may be initially inhibited by Fak to allow proper dendritic growth of dendrites and spines. During the tiling of dendrites from same types of neurons or self-avoidance of sister dendrites from same neurons, contact-dependent signaling from homophilic adhesion between Pcdhs may inhibit CAKs, thus activate RhoA, leading to dendritic and spine retraction. This mechanism may generate homophilic repulsion thought to be necessary for proper dendritic arborization and synaptic connections (Hattori et al., 2008; Jan and Jan, 2010; Zipursky and Sanes, 2010).

Indeed, Fak may be required for both dendritic growth (Schlomann et al., 2009) and spine stabilization (Shi et al., 2009). In cultured hippocampal neurons, αKO results in a significant increase in ADBL (Figure 1P), whereas *Fak* knockdown results in a decrease in the branch length and a slight increase in the number of filopodia, suggesting that the *Fak* knockdown leads to retraction of dendrites to filopodia in developing neurons (Supplementary Figure S7; Moeller et al., 2006). Consistently, αKO results in a significant decrease in the dendritic segment and spine numbers (Figure 2) and a slight increase in a membrane-associated active-form of Fak (Figure 8F) *in vivo*. Consistently, the *Fak* overexpression causes a slight increase in ADBL (data not shown) and TDBL (Figure 4J). This suggests that the α cluster regulates the dendritic branch length through Fak. The activation of Fak leads to inhibition of RhoA which controls the retraction of actin cytoskeleton in dendrites and spines through ROCK (Arthur et al., 2000; Ren et al., 2000; Tomar et al., 2009). Consistently, ROCK inhibition in combination with αKO and γKD results in a significant increase in ADBL (Figure 6H; Nakayama et al., 2000). Thus, the Pcdh-CAK-Rho GTPase pathway may be important to regulate dendritic and spine morphogenesis.

The *Pcdh* clusters and *CAKs* (*Pyk2* and *Fak*) could regulate both the long-term genetic programmed dendritic and spine development as well as the short-term activity-dependent dendritic and spine morphogenesis through Rho GTPases. The Pcdh-CAK-Rho GTPase pathway may be crucial for sculpting dendritic patterning and spine morphology to construct synaptic connections during brain development. Interestingly, the activation of Pyk2 is essential for induction of long-term potentiation (Huang et al., 2001) and of long-term depression (Hsin et al., 2010) in hippocampus. Given the calcium dependence of both Pcdh and Pyk2, it is intriguing that the Pcdh-CAK-Rho GTPase pathway may be important for a wide variety of calcium-dependent signaling events such as dendritic and spine plasticity in structural remodeling during learning and memory.

Downloaded from https://academic.oup.com/jmcb/article/4/6/362/849369 by guest on 16 August 2022

Materials and methods

Mice

The generation of *Pcdhα* cluster deletion and *Pcdhα-CFP* mice was previously described (Wu et al., 2007, 2008). The heterozygous *Pcdhα-CFP* mice were used to determine the expression patterns of *Pcdhα* cluster *in vivo*. Animals were maintained at 23°C in a 12-h (7:00–19:00) light and 12-h (19:00–7:00) dark schedule. All experiments are complied with the Institutional Animal Care and Use Committee under the relevant protocol.

Antibodies

The antibodies used mouse anti-FLAG M2 (Sigma), rabbit anti-CFP (Invitrogen), mouse anti-Myc (Millipore), rabbit anti-Pyk2 (Abcam and Invitrogen), rabbit anti-Tyr $(P)^{402}$-Pyk2 (Abcam), mouse anti-Fak (Santa Cruz), rabbit anti-Tyr $(P)^{397}$-Fak (Santa Cruz), rabbit anti-actin (Abcam), mouse anti-tubulin (Abcam), mouse anti-Rac1 (Millipore), mouse anti-RhoA (Cytoskeleton), rabbit anti-Pcdhα (Synaptic Systems), rabbit anti-Pcdhγ (Synaptic Systems and a kind gift from Graig Phillips), mouse anti-MAP2 (Sigma), rabbit anti-Tau (Abcam) and mouse anti-synaptophysin (Millipore). Alexa 488-Fluor and Cy3-conjugated secondary antibodies (Jackson ImmunoResearch and Invitrogen) were used for immunostaining.

Plasmid construction

The EGFP expression vector (*pEGFP-N2*) was generated from pIRES2-EGFP (Clontech) by replacing the IRES and EGFP-coding sequences with EGFP-coding sequences using *Bam*HI and *Not*I sites. The Flag-tag vector (pFlag) was created from pEGFP-N2 by replacing the EGFP-coding sequence with Flag tag sequences using *Sac*II/*Not*I sites. Full-length *Pcdhα1* cDNA was amplified by RT-PCR from total RNA isolated from mouse brain tissues and cloned into pFlag. The myristylated-α-CR (myr-α-CR) was created with PCR using the *Pcdhα1* plasmid as a template and cloned into pFlag using *Xho*I/*Sac*II sites. Myristylated Pcdh-γ-CR (myr-γ-CR) was amplified by RT-PCR and then cloned into pFlag vector. The sequences for the primers: atcggagctcgatacggaaagtgcagtac and aatgtcgacctggtcactgttgtccgtcg for *Pcdhα1*; tatctcgagccaccatgggcagtagcaagagcaagcctaaggaccccagccagcgccggcgtccccggcagcc caaccct and tccgcggtctggtcactgttgtccgtcgtg for myr-α-CR and tatctcgagccaccatgggcagtagcaagagcaagcctaaggaccccagccagcgccggcgtcaa gccccgcccaacact and atgatccgcggtcttcttctctttcttgcccg for myr-γ-CR.

We amplified full-length cDNA clones of *Pyk2*, *Fak*, *Rac1*, and *PcdhγC3* by RT-PCR from mouse brain tissues with primer pairs: atgaattcgaggatgtccggggtgtctga and atggatccccactctgcaggcgggtgg for *Pyk2*; gcgatatcatggcagctgcttatcttgaccca and atggatccacagtg tggccgtgtctgcc for *Fak*; tatctcgagatgcaggccatcaagtgtg and tcggaat tctgtacaacagcaggcattttctc for *Rac1*; tatgaattcatggtcgcagaggcccggag and cgcaagcttgtacttcttctctttcttgcccgatttctt for *PcdhγC3*. The amplified fragments were cloned into pcDNA-3.1 vector using *Hind*III/*Bam*HI sites for *Pyk2*, *Eco*RV/*Bam*HI sites for *Fak*, *Xho*I/*Eco*RI sites for *Rac1*, and *Eco*RI/*Hin*dIII sites for *PcdhγC3*. Pyk2 mutations at Y402F, K457A, Y579F, Y580F, and Y881F, and the constitutively active Rac1 mutation (Rac1V12) were constructed with *Pyk2* and *Rac1* plasmids using the QuikChange site-directed mutagenesis kit (Stratagene). All constructs were validated by sequencing. The primers were agagtcagacatctttgcggagattcccg and cgggaatctccgcaaagatgtctgactct for Pyk2 Y402F, ttaatgtggccgtcgcgacctgtaagaaagactgtacc and ggtacagtctttcttacaggtcgcgacggccacattaa for Pyk2 K457A, cattgaggacgagactttacaaagcctctgtg and cacagaggctttgtaaaagtcttcgtcctcaatg for Pyk2 Y579F, gagacgaagactatttcaaagcctctgtgacc and ggtcacagaggctttgaaatagtcttcgtcctc for Pyk2 Y580F, ccgatgacctcgtgttccacaatgtcatgac and gtcatgacattgtggaacacgaggtcatcgg for Pyk2 Y881F, ggtggtgggagacgtagctgttggtaaaacc and ggttttaccaacagctacgtctcccaccacc for Rac1V12.

For RNAi constructs, complementary oligo pairs for short hairpin (shRNA) sequences of *Pcdhγ*, *Pyk2*, and *Fak* were annealed and ligated into the pSilencer siRNA expression vector (Ambion) using *Hin*dIII/*Bam*HI sites.

Immunohistochemistry

After perfusion of mice with 4% ice-cold PFA, the brain was post-fixed for 24 h and equilibrated in 30% sucrose solution for another day. Free-floating coronal sections rinsed in PBS were blocked in 5% bovine serum albumin (BSA; Jackson ImmunoResearch), 0.1% Triton X-100 in PBS, for 1 h at 25°C. Anti-CFP antibodies were incubated overnight at 4°C. Alexa 488 Fluor-conjugated secondary antibody was incubated for 1 h at 25°C. Sections were imaged using a high-resolution digital camera (Axiocam) attached to a Zeiss microscope (Axiovert 200) driven by the AxioVision Software (Zeiss).

Preparation of total brain protein and crude membrane fraction, and western blot

Whole brain tissues were homogenized with the lysis buffer [50 mM Tris–HCl, pH 7.5, 150 mM NaCl, 1% NP40, 0.25% sodium deoxycholate, 10 mM NaF, 10 mM Na_3VO_4, 1 mM phenylmethanesulfonyl fluoride (PMSF), and protease inhibitors]. The debris was cleared by centrifugation at 12000*g* for 20 min at 4°C. The supernatants were used for protein quantification with the bicinchoninic acid assay method and for western blot or the Rho GTPase activation assay.

The crude membrane fraction was prepared as reported (Chen et al., 2009). In brief, the brain tissues were homogenized with a grinder in the buffer [50 mM Tris–HCl, pH 7.5, 150 mM NaCl, 1 mM ethylene diamine tetraacetic acid (EDTA), 1.5 mM $MgCl_2$, 10 mM NaF, 10 mM Na_3VO_4, 1 mM PMSF, and protease inhibitors]. The cell debris and nuclei were removed by low-speed centrifugation at 1000*g* for 20 min at 4°C. The supernatant was centrifuged by high-speed centrifugation at 16000*g* for 20 min at 4°C, and the resulting pellet was resuspended in buffer (50 mM Tris–HCl, pH 7.5, 150 mM NaCl, 1 mM EDTA, 1.5 mM $MgCl_2$, 10 mM NaF, 10 mM Na_3VO_4, 1 mM PMSF, 0.8% Triton X-100, and protease inhibitors) for protein quantification and western blot. IRDye680-conjugated goat anti-rabbit and IRDye800-conjugated goat anti-mouse secondary antibodies (both from Biosciences) were used for western blot. Signals were scanned on the Odyssey system (Li-Cor).

These western blot experiments were performed by using littermate mice and repeated for at least three times with similar results. Quantification was performed with the TotalLab Quant Software (TotalLab) and the results were normalized with tubulin, total membrane-associated Pyk2 or Fak, total Rac1 or RhoA, respectively. The significance of difference was assessed by the Student's *t*-test.

Rho GTPase activation assay

The activation of Rac1 was measured with a Rac1 activation assay kit (Millipore) and the activation of RhoA was measured

Downloaded from https://academic.oup.com/jmcb/article/4/6/362/849369 by guest on 16 August 2022

with a RhoA activation assay kit (Cytoskeleton) according to the manufacture's manuals. These small GTPase assays were each repeated at least three times with littermate mice.

Hippocampal neuron culture, transfection, and drug treatment

Hippocampi were collected from E18.5 embryos in Hanks' Balanced Salt Solution with 0.5% glucose, 10 mM Hepes, 100 μg/ml penicillin/streptomycin. Tissues were digested with 0.25% trypsin for 15 min at 37°C. After stopping the reaction with trypsin inhibitor (0.5 mg/ml) for 3 min at room temperature (RT), tissues were gently triturated in the plating medium [minimum essential medium (MEM), 10% fetal bovine serum (FBS), 1 mM glutamine, 10 mM Hepes, 50 μg/ml penicillin/streptomycin] until fully dissociated. Cell viability and density was determined using 0.4% trypan blue and a hemacytometer. Cells were plated at the density of 1000 cells/mm^2 for 7 DIV or 500 cells/mm^2 for 14 DIV neurons onto 4-well or 8-well Lab-Tek II chamber slides (Nunc) sequentially precoated with 100 μg/ml poly-L-lysine (Sigma) and 5 μg/ml laminin (Invitrogen). Cells were incubated with 5% CO_2 at 37°C. After 3–4 h, the plating medium was replaced with a serum-free culture medium (Neurobasal medium, 2% B27, 0.5 mM glutamine, 50 μg/ml penicillin/streptomycin supplemented with 25 μM glutamate), and thereafter half of the medium (W/O glutamate) was replaced twice a week. For 14 DIV culture, 2 mM cytosine arabinoside (Sigma) was added at day 3 to inhibit the proliferation of glia.

Neurons were transfected with mock and experimental plasmids at 5 or 12 DIV using a calcium phosphate transfection kit (Invitrogen) and were cultured until 7 or 14 DIV to be fixed for analyses. For drug treatment, the Rac1-specific inhibitor NSC23766 or ROCK-specific inhibitor Y-27632 (Calbiochem) or the control mock solvent was added 3 h after transfection at final concentrations of 15 and 50 μM, respectively.

Immunofluorescent staining

Cultured primary hippocampal neurons were washed once with 1× PBS, fixed in 4% PFA for 20 min at RT, washed and permeabilized with 0.3% Triton X-100 for 10 min. After blocking with 5% BSA, cells were incubated with primary antibodies at 4°C overnight. Signals were detected with Cy3- or Alexa 488 Fluor-conjugated secondary antibodies. Cell nuclei were visualized with DAPI.

Image analysis and quantification

The quantification of the TDBL, TDBTN, ADBL, number of primary dendrites, and Sholl analysis were done on images taken with the 20× objective (Zeiss Plan-Neofluar). The dendritic tree of each neuron was traced in Image J (NIH). The resulting trace was used to calculate the parameters. For Sholl analyses, a series of concentric circles with 25 μm intervals were drawn around soma, and crossings of dendrites with each circle were counted automatically by a Sholl analysis plugin (from the Anirvan Ghosh lab). The filopodia per 10 μm dendritic segment were quantified with images captured with the 100× oil immersion objective. The filopodia were defined as headless protrusion >3 μm but <10 μm.

In mature neuron, the spine density (spine numbers per 10 μm dendritic segment), spine length, and spine width (diameter of spine head) of secondary branches were quantified on images acquired with the 100× oil immersion objective. The spines were defined as a typical headed protrusion of any length up to 3 μm or a headless dendritic protrusion of 1–3 μm long.

The neuronal culture and transfection experiments were performed at least three times with 4 or 6 hippocampi of littermate mice from different dams for each experiment. The reliability of the measurements was examined by comparing results obtained by two independent observers with almost identical results. The experiments were carried out in a double-blind fashion with respect to genotypes of homozygous and control littermate mice or with respect to transfection of experimental or mock plasmids. For Sholl analysis in hippocampal cultures, only neurons with more than three primary dendrites were used to reduce variations. All of the primary hippocampal cultured neurons were quantified from at least three sets of homozygous and control littermate mice with two or three pups per genotype each time. The data were presented as the mean ± SEM. Unpaired two-tailed Student's *t*-test was used to assess the significance of difference from controls.

Golgi staining and 3D reconstruction of CA1 pyramidal neurons

Golgi staining experiments were performed by using the Rapid Golgistain Kit according to its manual (FD Neuron Technologies). Briefly, homozygous and wild-type P15 littermate mice were deeply anesthetized and sacrificed. The brain was removed as quickly as possible and put into the impregnation solution of equal volume mixture of Solutions A and B for 8 days. The impregnation solution was then replaced by the Solution C for another 4 days. The brain was then cut into 150 μm sections using a cryostat (Leica CM3050S). The sections were washed twice and immersed in the 1:1 mixture of Solutions D and E for 10 min. After dehydration, the sections were cleared in xylene and coverslipped with the mounting medium (Permount).

Images were collected with an Olympus confocal microscopy (FV-1000) under a 20× objective for dendritic analyses and imported into the Neuromantic software (www.reading.ac.uk/neuromantic). Each CA1 pyramidal neuron was 3D reconstructed by tracing the dendritic paths of the Z-stacking pictures. The number of branch points (bifurcations) and of segments between branch points were analyzed automatically by the software and checked manually. The reconstructed neurons were imported into the Image J (NIH) for the Sholl analysis.

For spine analyses, high resolution images were collected under a 60× oil objective (NA 1.35) with a 3× digital zooming factor. The reconstructed Z-stacking pictures were imported into the Image J (NIH). The spine density, spine length and width were analyzed manually on 20–30 μm long basal dendritic segments from CA1 hippocampal neurons. The experimenter and analyzer were blinded to genotyping until all data were collected and analyzed.

Cell culture, transfection, and western blot

HEK293 cells were maintained in MEM with 10% FBS, 4 mM L-glutamine and 100 μg/ml penicillin/streptomycin. Cultured cells were transfected with experimental or mock plasmids using Lipofectamine 2000 (Invitrogen). Cells were lysated with the lysis buffer at 48 h after transfection, and the debris was cleared by centrifugation at 12000*g* for 20 min at 4°C. The supernatant was used for western blot or Rho GTPase activation assay as described above. The western blot experiments were repeated

Downloaded from https://academic.oup.com/jmcb/article/4/6/362/849369 by guest on 16 August 2022

for at least three times with similar results. Quantification was performed as described above.

Addendum

While this manuscript was in revision, A.M. Garrett, D. Schreiner, M.A. Lobas, and J.A. Weiner (2012, γ-protocadherins control cortical dendrite arborization by regulating the activity of a FAK/PKC/MARCKS signaling pathway. Neuron 74:269–276) reported a critical role of the γ cluster in dendrite arborization in a mouse cortex through a FAK-PKC-MARCKS pathway.

Supplementary material

Supplementary material is available at *Journal of Molecular Cell Biology* online.

Acknowledgements

We wish to thank Dr Graig Phillips (NYU) for the Pcdhγ antibody. We thank Drs Zheng Li (NIH), Liqun Luo (Stanford), Joshua Weiner (U of Iowa) and Xiang Yu (ION) for suggestions.

Funding

This work was supported by grants to Q.W. from the Ministry of Science and Technology of China (2009CB918700), the National Natural Science Foundation (31171015, 30970669), the Science and Technology Commission of Shanghai Municipality (09PJ1405300). Q.W. is a Pujiang Investigator. M.R.C. is an Investigator of Howard Hughes Medical Institute.

Conflict of interest: none declared.

References

Arthur, W.T., Petch, L.A., and Burridge, K. (2000). Integrin engagement suppresses RhoA activity via a c-Src-dependent mechanism. Curr. Biol. *10*, 719–722.

Avraham, H., Park, S.Y., Schinkmann, K., et al. (2000). RAFTK/Pyk2-mediated cellular signalling. Cell. Signal. *12*, 123–133.

Burridge, K., and Wennerberg, K. (2004). Rho and Rac take center stage. Cell *116*, 167–179.

Cajal, S.R. (1909). Histology of the Nervous System of Man and Vertebrates. New York: Oxford University Press.

Chen, J., Lu, Y., Meng, S., et al. (2009). Alpha- and gamma-protocadherins negatively regulate PYK2. J. Biol. Chem. *284*, 2880–2890.

Derkinderen, P., Toutant, M., Burgaya, F., et al. (1996). Regulation of a neuronal form of focal adhesion kinase by anandamide. Science *273*, 1719–1722.

Dikic, I., Tokiwa, G., Lev, S., et al. (1996). A role for Pyk2 and Src in linking G-protein-coupled receptors with MAP kinase activation. Nature *383*, 547–550.

Girault, J.A., Costa, A., Derkinderen, P., et al. (1999). FAK and PYK2/CAKbeta in the nervous system: a link between neuronal activity, plasticity and survival? Trends Neurosci. *22*, 257–263.

Govek, E.E., Newey, S.E., and Van Aelst, L. (2005). The role of the Rho GTPases in neuronal development. Genes Dev. *19*, 1–49.

Han, M.H., Lin, C., Meng, S., et al. (2010). Proteomics analysis reveals overlapping functions of clustered protocadherins. Mol. Cell. Proteomics *9*, 71–83.

Hasegawa, S., Hamada, S., Kumode, Y., et al. (2008). The protocadherin-alpha family is involved in axonal coalescence of olfactory sensory neurons into glomeruli of the olfactory bulb in mouse. Mol. Cell. Neurosci. *38*, 66–79.

Hattori, D., Millard, S.S., Wojtowicz, W.M., et al. (2008). Dscam-mediated cell recognition regulates neural circuit formation. Annu. Rev. Cell Dev. Biol. *24*, 597–620.

Hsin, H., Kim, M.J., Wang, C.F., et al. (2010). Proline-rich tyrosine kinase 2 regulates hippocampal long-term depression. J. Neurosci. *30*, 11983–11993.

Huang, Y., Lu, W., Ali, D.W., et al. (2001). CAKbeta/Pyk2 kinase is a signaling link for induction of long-term potentiation in CA1 hippocampus. Neuron *29*, 485–496.

Hyman, S.E. (2008). A glimmer of light for neuropsychiatric disorders. Nature *455*, 890–893.

Jan, Y.N., and Jan, L.Y. (2010). Branching out: mechanisms of dendritic arborization. Nat. Rev. Neurosci. *11*, 316–328.

Katori, S., Hamada, S., Noguchi, Y., et al. (2009). Protocadherin-γ family is required for serotonergic projections to appropriately innervate target brain areas. J. Neurosci. *29*, 9137–9147.

Kohmura, N., Senzaki, K., Hamada, S., et al. (1998). Diversity revealed by a novel family of cadherins expressed in neurons at a synaptic complex. Neuron *20*, 1137–1151.

Konur, S., and Ghosh, A. (2005). Calcium signaling and the control of dendritic development. Neuron *46*, 401–405.

Lamprecht, R., and LeDoux, J. (2004). Structural plasticity and memory. Nat. Rev. Neurosci. *5*, 45–54.

Lamprecht, R., Farb, C.R., and LeDoux, J.E. (2002). Fear memory formation involves p190 RhoGAP and ROCK proteins through a GRB2-mediated complex. Neuron *36*, 727–738.

Lefebvre, J.L., Zhang, Y., Meister, M., et al. (2008). Gamma-protocadherins regulate neuronal survival but are dispensable for circuit formation in retina. Development *135*, 4141–4151.

Lev, S., Moreno, H., Martinez, R., et al. (1995). Protein tyrosine kinase PYK2 involved in Ca^{2+}-induced regulation of ion channel and MAP kinase functions. Nature *376*, 737–745.

Lietha, D., Cai, X., Ceccarelli, D.F., et al. (2007). Structural basis for the autoinhibition of focal adhesion kinase. Cell *129*, 1177–1187.

Lin, Y.C., and Koleske, A.J. (2010). Mechanisms of synapse and dendrite maintenance and their disruption in psychiatric and neurodegenerative disorders. Annu. Rev. Neurosci. *33*, 349–378.

Luo, L., Hensch, T.K., Ackerman, L., et al. (1996). Differential effects of the Rac GTPase on Purkinje cell axons and dendritic trunks and spines. Nature *379*, 837–840.

Moeller, M.L., Shi, Y., Reichardt, L.F., et al. (2006). EphB receptors regulate dendritic spine morphogenesis through the recruitment/phosphorylation of focal adhesion kinase and RhoA activation. J. Biol. Chem. *281*, 1587–1598.

Murata, Y., Hamada, S., Morishita, H., et al. (2004). Interaction with protocadherin-gamma regulates the cell surface expression of protocadherin-alpha. J. Biol. Chem. *279*, 49508–49516.

Nakayama, A.Y., Harms, M.B., and Luo, L. (2000). Small GTPases Rac and Rho in the maintenance of dendritic spines and branches in hippocampal pyramidal neurons. J. Neurosci. *20*, 5329–5338.

Pedrosa, E., Stefanescu, R., Margolis, B., et al. (2008). Analysis of protocadherin alpha gene enhancer polymorphism in bipolar disorder and schizophrenia. Schizophr. Res. *102*, 210–219.

Phillips, G.R., Tanaka, H., Frank, M., et al. (2003). Gamma-protocadherins are targeted to subsets of synapses and intracellular organelles in neurons. J. Neurosci. *23*, 5096–5104.

Ren, X.D., Kiosses, W.B., Sieg, D.J., et al. (2000). Focal adhesion kinase suppresses Rho activity to promote focal adhesion turnover. J. Cell Sci. *113*, 3673–3678.

Schaller, M.D. (2010). Cellular functions of FAK kinases: insight into molecular mechanisms and novel functions. J. Cell Sci. *123*, 1007–1013.

Schlaepfer, D.D., Hanks, S.K., Hunter, T., et al. (1994). Integrin-mediated signal transduction linked to Ras pathway by GRB2 binding to focal adhesion kinase. Nature *372*, 786–791.

Schlomann, U., Schwamborn, J.C., Müller, M., et al. (2009). The stimulation of dendrite growth by Sema3A requires integrin engagement and focal adhesion kinase. J. Cell Sci. *122*, 2034–2042.

Schreiner, D., and Weiner, J.A. (2010). Combinatorial homophilic interaction between gamma-protocadherin multimers greatly expands the molecular diversity of cell adhesion. Proc. Natl Acad. Sci. USA *107*, 14893–14898.

Scott, E.K., and Luo, L. (2001). How do dendrites take their shape? Nat. Neurosci. *4*, 359–365.

Shapiro, L., and Colman, D.R. (1999). The diversity of cadherins and implications for a synaptic adhesive code in the CNS. Neuron *23*, 427–430.

Downloaded from https://academic.oup.com/jmcb/article/4/6/362/849369 by guest on 16 August 2022

Shi, Y., Pontrello, C.G., DeFea, K.A., et al. (2009). Focal adhesion kinase acts downstream of EphB receptors to maintain mature dendritic spines by regulating cofilin activity. J. Neurosci. *29*, 8129–8142.

Singh, S.M., Castellani, C., and O'Reilly, R. (2009). Autism meets schizophrenia via cadherin pathway. Schizophr. Res. *116*, 293–294.

Sperry, R.W. (1963). Chemoaffinity in the orderly growth of nerve fiber patterns and connections. Proc. Natl Acad. Sci. USA *50*, 703–710.

Takeichi, M. (2007). The cadherin superfamily in neuronal connections and interactions. Nat. Rev. Neurosci. *8*, 11–20.

Tasic, B., Nabholz, C.E., Baldwin, K.K., et al. (2002). Promoter choice determines splice site selection in protocadherin alpha and gamma pre-mRNA splicing. Mol. Cell *10*, 21–33.

Tomar, A., and Schlaepfer, D.D. (2009). Focal adhesion kinase: switching between GAPs and GEFs in the regulation of cell motility. Curr. Opin. Cell Biol. *21*, 676–683.

Tomar, A., Lim, S.T., Lim, Y., et al. (2009). A FAK-p120RasGAP-p190RhoGAP complex regulates polarity in migrating cells. J. Cell Sci. *122*, 1852–1862.

Van Aelst, L., and Cline, H.T. (2004). Rho GTPases and activity-dependent dendrite development. Curr. Opin. Neurobiol. *14*, 297–304.

Wang, X., Su, H., and Bradley, A. (2002a). Molecular mechanisms governing Pcdh-gamma gene expression: evidence for a multiple promoter and cis-alternative splicing model. Genes Dev. *16*, 1890–1905.

Wang, X., Weiner, J.A., Levi, S., et al. (2002b). Gamma protocadherins are required for survival of spinal interneurons. Neuron *36*, 843–854.

Wu, Q. (2005). Comparative genomics and diversifying selection of the clustered vertebrate protocadherin genes. Genetics *169*, 2179–2188.

Wu, Q., and Maniatis, T. (1999). A striking organization of a large family of human neural cadherin-like cell adhesion genes. Cell *97*, 779–790.

Wu, Q., Zhang, T., Cheng, J.F., et al. (2001). Comparative DNA sequence analysis of mouse and human protocadherin gene clusters. Genome Res. *11*, 389–404.

Wu, S., Ying, G., Wu, Q., et al. (2007). Toward simpler and faster genome-wide mutagenesis in mice. Nat. Genet. *39*, 922–930.

Wu, S., Ying, G., Wu, Q., et al. (2008). A protocol for constructing gene targeting vectors: generating knockout mice for the cadherin family and beyond. Nat. Protoc. *3*, 1056–1076.

Yagi, T., and Takeichi, M. (2000). Cadherin superfamily genes: functions, genomic organization, and neurologic diversity. Genes Dev. *14*, 1169–1180.

Ye, B., and Jan, Y.N. (2005). The cadherin superfamily and dendrite development. Trends Cell Biol. *15*, 64–67.

Yu, X., and Malenka, R.C. (2003). Beta-catenin is critical for dendritic morphogenesis. Nat. Neurosci. *6*, 1169–1177.

Zipursky, S.L., and Sanes, J.R. (2010). Chemoaffinity revisited: Dscams, protocadherins, and neural circuit assembly. Cell *143*, 343–353.

Zou, C., Huang, W., Ying, G., et al. (2007). Sequence analysis and expression mapping of the rat clustered protocadherin gene repertoires. Neuroscience *144*, 579–603.

Zrihan-Licht, S., Fu, Y., Settleman, J., et al. (2000). RAFTK/Pyk2 tyrosine kinase mediates the association of p190 RhoGAP with RasGAP and is involved in breast cancer cell invasion. Oncogene *19*, 1318–1328.

Downloaded from https://academic.oup.com/jmcb/article/4/6/362/849369 by guest on 16 August 2022